GEOPHYSICAL RESEARCH LETTERS, VOL. 39, L19309, doi:10.1029/2012GL053518, 2012

Magma mobilization by downward-propagating decompression of the Eyjafjallajökull volcanic plumbing system

Jon Tarasewicz,[1] Robert S. White,[1] Andrew W. Woods,[2] Bryndís Brandsdóttir,[3] and Magnús T. Gudmundsson[3]

Received 8 August 2012; revised 11 September 2012; accepted 14 September 2012; published 13 October 2012.

[1] Detailed observations of the 2010 Eyjafjallajökull eruptions in Iceland show seismic activity propagating vertically through the entire crust during a ten-week period of volcanic unrest comprising multiple eruption episodes. Systematic changes in magma chemistry suggest a complex magmatic plumbing system, tapping several accumulation zones at different depths containing magma of differing ages and compositions. During the eruption, a systematic downward propagation of seismicity through the crust and into the upper mantle to ~30 km depth occurred in a series of steps, each of which preceded an explosive surge in eruption rate. Here we show that the sequence of seismicity and eruptive activity may be explained by the downward propagation of a decompression wave that triggers magma release from progressively deeper sills in the crust. Comparing observations of the downward-propagating seismicity with the decompression of a series of model elastic sills suggests that each sill was 1–10 km^3 in size. **Citation:** Tarasewicz, J., R. S. White, A. W. Woods, B. Brandsdóttir, and M. T. Gudmundsson (2012), Magma mobilization by downward-propagating decompression of the Eyjafjallajökull volcanic plumbing system, *Geophys. Res. Lett.*, *39*, L19309, doi:10.1029/2012GL053518.

1. Introduction

[2] The 2010 eruptions of Eyjafjallajökull in Iceland culminated, after nearly two decades of intermittent magmatic unrest, in the opening of a flank fissure during 20 March to 12 April. This was followed, after a two-day hiatus, by an explosive eruption from the summit caldera during 14 April to mid-June 2010 (yellow stars, Figure 1). Over several preceding months, melt flow of ~0.05 km^3 from depth inflated a shallow magma chamber at ~5 km beneath the eastern flank [*Sigmundsson et al.*, 2010]. Thousands of microearthquakes under the northeast flank of Eyjafjallajökull during March 2010 accompanied this intrusive activity [*Tarasewicz et al.*, 2012]. As the melt rose to inflate the shallow intrusion, it may also have intruded new sills at depth in the crust and intersected, or come close to, pre-existing intrusions such as those inferred from seismicity and surface deformation during the 1990s [*Sturkell et al.*, 2003; *Hjaltadóttir et al.*, 2009]. During the three-week flank eruption, only negligible deflation was observed geodetically. A change in magma compressibility in the magma chamber, caused by volatile exsolution as the chamber empties, may account for a mismatch between the extruded volume and the observed deflation of the source magma chamber in some settings [*Rivalta and Segall*, 2008]. However, geobarometric analyses indicate that the Eyjafjallajökull mafic flank magma partially crystallized at 16–18 km depth [*Keiding and Sigmarsson*, 2012], and the extruded volume of lava in the flank eruption was equivalent to almost half the pre-eruption intrusion volume (~0.05 km^3). Hence, it is likely that the lack of observed deflation is explained by the mafic flank magma having a deeper source than the shallow intrusion and either bypassing the shallow magma chamber, or flowing through it but counterbalancing the volume erupted from it with inflow of fresh magma during the eruption [*Sigmundsson et al.*, 2010; *Gudmundsson et al.*, 2012a].

[3] The subsequent summit eruption, 8 km west of the flank eruption site, began with mixed mafic and evolved melts from 14–18 April [*Sigmarsson et al.*, 2011; *Magnússon et al.*, 2012]. Accompanying seismicity suggests that the magma source was a separate, pre-existing magma chamber at ~5 km depth, directly beneath the summit [*Tarasewicz et al.*, 2012], (Figure 2). This contained highly evolved silicic melt, with the eruption triggered by injection of mafic melt [*Sigmarsson et al.*, 2011]. During this first explosive phase of the summit eruption, deflation of the shallow magma chamber was observed geodetically [*Sigmundsson et al.*, 2010], suggesting that magma supply from depth had ceased or was insufficient to keep the chamber fully replenished.

[4] The first explosive phase relieved much of the overpressure in the summit magma chamber. For two weeks from 19 April the eruption rate was substantially lower (Figure 2c), with mostly effusive lava flows, only limited explosive activity and little seismicity except in the shallowest few kilometers (Figure 2). Continued slow eruption gradually depressurized the summit magma chamber further. In addition, removal of mass by melting ~200 m of overlying ice from the summit region [*Magnússon et al.*, 2012] incrementally depressurized the shallow magma chamber, although this mass loss was partly counterbalanced by fresh ash and lava deposition around the summit (Figure 2a). Nonetheless, the confining pressure at the open vent of the magma conduit, and hence the pressure on melt in the conduit, would have been reduced by ~2 MPa by removing ~200 m of ice, regardless of fresh ash deposits elsewhere around the summit.

[5] A second explosive phase started 5 May, including three notable episodes (A, B, C in Figure 2). Each explosive eruptive episode lasted 1–2 days and was preceded by localized seismicity at depths of 10–13 km, ~19 km and ~24 km respectively (red stars, Figure 2d). The composition

[1]Bullard Laboratories, University of Cambridge, Cambridge, UK.
[2]BP Institute, University of Cambridge, Cambridge, UK.
[3]Institute of Earth Sciences, University of Iceland, Reykjavík, Iceland.

Corresponding author: J. Tarasewicz, Bullard Laboratories, University of Cambridge, Madingley Road, Cambridge CB3 0EZ, UK. (jptt2@cam.ac.uk)

0094-8276/12/2012GL053518

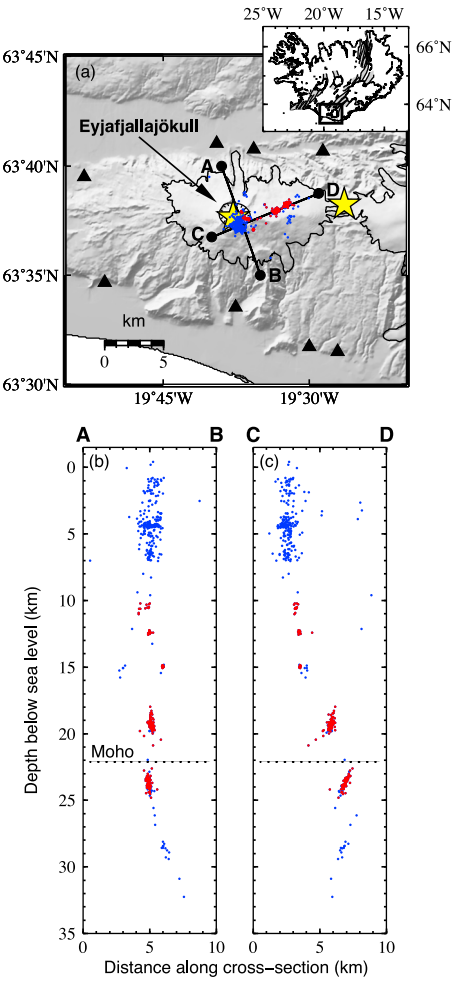

Figure 1. Location map. (a) Epicenters of 502 microearthquakes (blue and red dots) recorded 13 April to 17 May 2010 during the summit eruption. Red dots highlight 220 earthquakes deeper than 10 km that form a downward-propagating series of clusters; blue dots show all other events during the period for context. Black triangles are seismometer locations, thin black lines are extent of glaciers, yellow stars are eruption sites (eastern star – fissure eruption at Fimmvörðuháls, March 2010; western star – Eyjafjallajökull summit explosive eruption, April–May 2010). Inset: map of Iceland showing fissure swarms (grey) along volcanic systems. (b and c) Cross-sections along A–B and C–D respectively, showing depth distribution of seismicity from orthogonal viewpoints. No vertical exaggeration. Earthquakes were located using three-component digital seismic data from eight stations in the South Iceland Lowland network and six temporary stations deployed by the University of Iceland. Hypocenters were found initially using an automatic Coalescence Microseismic Mapping technique [*Drew*, 2010; *Tarasewicz et al.*, 2012] then refined by manually picking P- and S-wave arrival times and applying the HypoDD double-difference relative relocation algorithm [*Waldhauser and Ellsworth*, 2000]. Mean relative location uncertainties reported by HypoDD in the highlighted red clusters are 49 m vertically and 28 m horizontally.

of erupted material changed, suggesting that it was no longer sourced solely from the shallow summit magma chamber that fed the first explosive phase. The mafic component of the melt became more primitive, but formed a smaller proportion of the melt, whilst the silicic component became less evolved but formed a greater proportion of the melt than during the first explosive phase [*Sigmarsson et al.*, 2011] (Figure 2b). Both mafic and silicic components continued to evolve during the second explosive phase after 5 May.

2. Decompression of the Magmatic Plumbing System

[6] We suggest that at some critical threshold, depressurization of the summit magma chamber began to affect the deeper magmatic plumbing system. This prompted mobilization of magma from sill A at 10–13 km depth (Figure 3) and caused seismogenic fracturing as melt escaped into the conduit, starting 2 May. The sill is likely already to have been overpressured because it would have been emplaced at (or possibly greater than) lithostatic pressure before the eruptions. Further overpressuring may have occurred after emplacement by fractionation, volatile exsolution, or injection of small amounts of juvenile magma as the volcano inflated before the eruptions.

[7] We propose that several factors increased the sill's overpressure during the eruption, causing it to become critically overpressured and allowing melt to 'burst' into the conduit up to the surface. First, relaxation of elastic stresses in the crust surrounding the summit magma chamber as it deflated reduced the confining stresses on sill A beneath (Figure 3 and Figure S1 in the auxiliary material).[1] Second, the conduit from the summit chamber to depth became progressively underpressured at depth with respect to sill A. This created a pressure gradient across the rock between the sill and the conduit, possibly where an earlier feeder for the sill had been. Plugs of solidified material shunting along such a feeder or up the conduit may generate seismicity as melt escapes [*White et al.*, 2011; *White et al.*, 2012]. Third, approximately one-third of the mass erupted from the summit chamber before 5 May was advected away from Iceland via the ash plume, and a substantial amount of the remaining mass deposited in Iceland fell outside the summit caldera [*Gudmundsson et al.*, 2012a, 2012b]. This reduced the lithostatic load above sill A, although the elastic strength of the crust moderated this effect at depth. An overpressure in the sill of order 1–5 MPa would be sufficient to cause fracturing into the nearby conduit, which provided the path of least resistance. Given the likely pre-existing overpressure in the sill, even a small incremental increase in overpressure could have triggered escape of melt into the conduit.

[8] After seismicity at 10–13 km depth began on 2 May, GPS data indicate re-inflation of the summit magma chamber (3–6 May) [*Gudmundsson et al.*, 2012a, 2012b] starting before the second phase of explosive eruptive activity on 5 May. We interpret this as overpressured melt from sill A rising up the conduit into the summit chamber and causing renewed explosive surface activity. Subsequently, depressurization of sill A as magma was removed caused the underlying sill B (Figure 3) to become critically overpressured by the same

[1]Auxiliary materials are available in the HTML. doi:10.1029/2012GL053518.

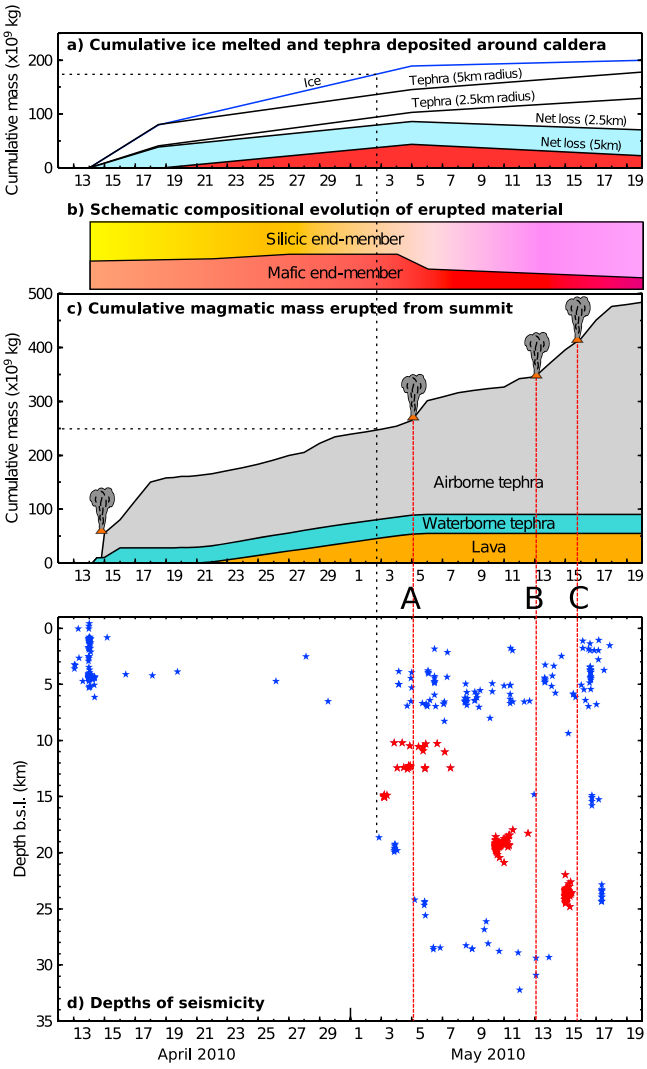

Figure 2. Time series of summit eruption 14 April to 20 May 2010. (a) Cumulative ice mass melted and tephra mass deposited in summit region [*Gudmundsson et al.*, 2012a, 2012b]. 'Net loss' curves indicate the net mass loss within 2.5 km (blue shading) and 5.0 km (red shading) from the center of the caldera. (b) Schematic compositional evolution of erupted products from magma mingling of mafic and silicic end-members, which themselves evolve with time [*Sigmarsson et al.*, 2011]. (c) Cumulative magmatic mass erupted. Cartoon volcanoes indicate significant bursts of explosive activity [*Gudmundsson et al.*, 2012a, 2012b]. (d) Depth of microearthquakes. Red clusters are those shown in red in Figure 1. Clusters occur progressively deeper, preceding explosive eruptions A, B, C. Black dashed line highlights onset of seismicity deeper than 10 km. Red dashed lines show onsets of resurgence in explosive activity.

mechanisms. Again, a swarm of deep seismicity, now at ~19 km depth (10 May), was followed two days later by a resurgence in explosive eruption. The process repeated as the decompression wave propagated down through the crust and finally mobilized melt stored in sill C, causing seismicity at ~24 km depth (15 May) followed by another explosive surface episode (Figure 2). After this final burst on 15–17 May, no further deep seismicity or intense explosive activity occurred; the overpressure in sills close to the conduit had been relieved and fresh melt supply from depth reduced or stopped.

[9] Out of the total of 270 earthquakes deeper than 10 km, 220 of them occurred in the sequence of clusters highlighted in red in Figures 1 and 2d. Of those that did not, many are spatially co-located with the events in red clusters at ~24 km and ~15 km depth, but occur later, perhaps as sills at those depths continued to drain after their initial burst. A few events occur at ~19 km and ~25 km depth several days before the major clusters occur at those depths, as well as some events at even greater depth during 6–14 May (Figure 2d). These events may indicate that the system is more complex than our simple conceptual model, but they may also be a response to decompression of sill A and the summit magma chamber that is consistent with the model. Deeper parts of the plumbing system may begin to 'creak' but melt cannot flow significantly, with an associated large seismic swarm, until the system above has decompressed more fully.

[10] The concomitant change in erupted composition at the start of the second explosive phase on 5 May may reflect the introduction of melt from sill A, which could be the source of the less-evolved silicic component that started to erupt at this time [*Sigmarsson et al.*, 2011]. In addition, magma from sill A, and subsequently sills B and C, may have mixed with magma residing in the conduit (initially mafic), the summit magma chamber (highly evolved silicic, plus mafic), and with magma derived from melting the country rock surrounding the summit chamber (silicic) [*Sigmarsson et al.*, 2011]. The complex evolution of melt compositions could be explained by contributions from multiple magma sources with residence times spanning days to decades at a range of storage depths in the crust and upper mantle [*Hjaltadóttir et al.*, 2009; *Sigmarsson et al.*, 2011; *Keiding and Sigmarsson*, 2012].

[11] Each eruption episode A, B and C discharged ~0.01–0.02 km^3 magma [*Gudmundsson et al.*, 2012a, 2012b]. Assuming an effective elastic bulk modulus of 10^9–10^{10} Pa implies sill volumes of order 1–10 km^3, if the initial overpressure in the sills at the point when melt escapes is of order 1–5 MPa, and assuming the erupted mass is equivalent to that removed from each sill.

[12] Seismicity associated with episodes A, B and C (Figure 2) occurred in the normally ductile part of the crust. However, brittle failure at depth can occur if strain rates are sufficiently high, such as may be caused by magma migration. Magma movement in the mid to lower crust is observed from microseismicity elsewhere in Iceland [*White et al.*, 2011; *Key et al.*, 2011] and sills at multiple depths in the crust and upper mantle are required on petrologic grounds [*Kelley and Barton*, 2008].

[13] To illustrate the effects of decompression, we consider three elastic sills beneath a near-surface magma chamber from which a vertical dike extends to the surface and to depth. This simple model approximates the summit magma chamber and sills A, B and C (Figure 3), before those sills have 'burst' into the conduit.

[14] We model the evolution of pressure in each sill and flow to the surface by assuming that the sills deform elastically and that flow is controlled by viscous stress in the conduit and the pressure difference between vertically adjacent sills. We assume that magma in a sill is mobilized at a critical

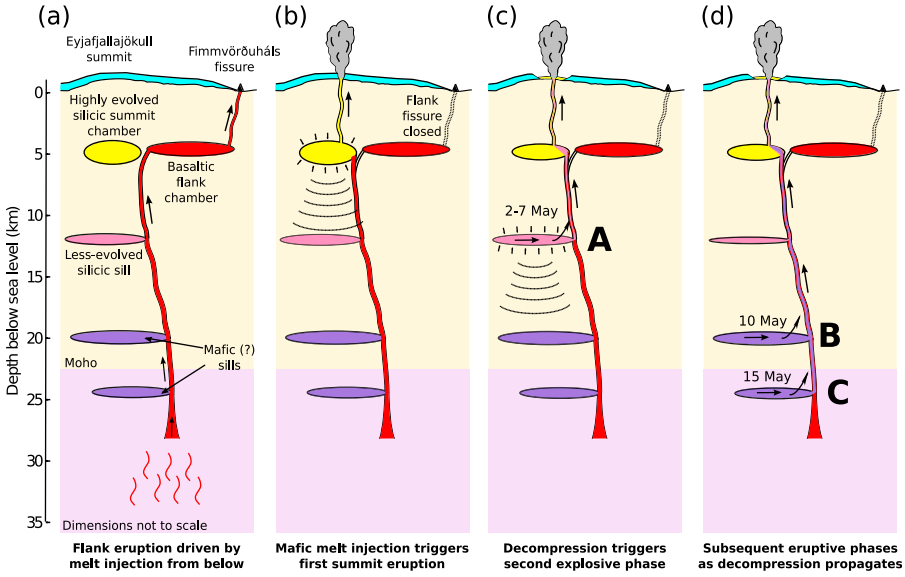

Figure 3. Cartoon illustrating melt sources during eruption. (a) Fimmvörðuháls flank eruption. During January–March 2010, low-viscosity, mafic melt flows up conduit from depth and inflates the eastern volcano flank, without extensive mixing with deeper sills. Fissure eruption of alkali basalt starts 20 March. Mafic melt continues to flow into flank chamber; no deflation observed geodetically [*Sigmundsson et al.*, 2010]. (b) Fissure eruption ends 12 April. Summit eruption starts 14 April, triggered by mafic melt injecting into evolved silicic melt in magma chamber beneath summit crater [*Sigmarsson et al.*, 2011]. Explosive activity subsides into effusive lava eruption. (c) Depressurization of shallow summit chamber causes melt mobilization at 10–15 km depth starting 2 May. Resurgence in explosive activity on 5 May ('A' in Figure 2), incorporates melt from sill at 10–15 km depth and fresh, primitive melt residing in the conduit. (d) Subsequent decompression wave mobilizes melt at ~19 km (10 May), and then ~24 km depth (15 May), causing seismic swarms as melt escapes from sills. Eruptions ('B' and 'C' in Figure 2) follow each burst of deep seismicity, lagging by 1–3 days. Eruption dies down as mafic melt supply reduces and overpressure in deep sills is relieved.

overpressure relative to the overlying decompressed system, which drives flow towards the surface via the conduit. This leads to equations of the form:

$$\frac{dp_i}{dt} = \frac{\beta}{V_i}\left[Q_i^{in} - Q_i^{out}\right]$$
$$Q_i^{in} = \lambda\frac{\pi r^4}{\mu_i}\left[\frac{p_{i+1} - p_i}{H_{i+1} - H_i}\right]; Q_i^{out} = \lambda\frac{\pi r^4}{\mu_{i-1}}\left[\frac{p_i - p_{i-1}}{H_i - H_{i-1}}\right]$$

where subscript i denotes one of the sills, A, B or C, i-1 denotes the overlying sill and $i+1$ the underlying sill. H, V and p are depth, volume and overpressure for each sill respectively. Q is flow rate in or out of the sill, μ is magma viscosity, β is bulk modulus of the surrounding crust and t is time. The dike radius, r, and λ, a shape factor for flow in the dike, are taken to be constant for simplicity. Below the deepest sill, C, we assume that there is no inflow. Outflow from the dike at the level of the shallowest sill, A, is assumed to go directly through the near-surface magma chamber to the surface.

[15] From the point at which sill A becomes critically overpressured and 'bursts' into the conduit, solution of these idealized coupled equations (Figure 4) shows that as melt moves out of sill A, the sill's overpressure, p_A, falls. As p_A continues to fall, sill B becomes critically overpressured and starts to erupt. This reduces the overpressure in sill B, which in turn triggers sill C to erupt. The precise timing of successive episodes (i.e., A, B and C) depends on the viscosity of magma in each sill, the overpressure of each sill, and the critical overpressure at which magma 'bursts' from the sill into the dike. In the illustrative calculation (Figure 4) we use a viscosity of 10,000 Pa s and an overpressure of 4 MPa.

[16] Volatiles exsolve as magma ascends and decompresses. Carbon dioxide may exsolve at depths of 15–20 km

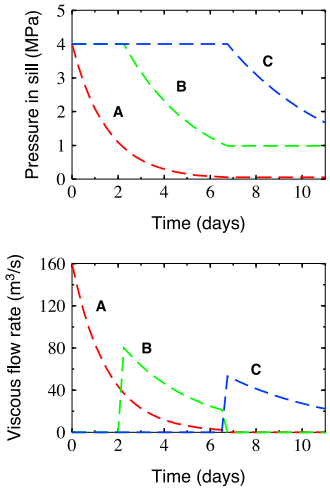

Figure 4. Pressure and flow rate evolution of modeled elastic sills. (top) Pressure evolution of sills assuming initial overpressure of 4 MPa, starting from the point at which the shallowest sill (A in Figure 3) becomes critically overpressured and melt escapes up the conduit. (bottom) Evolution of viscous flow rate out of each modeled sill, coupled to the pressure evolution shown in the top plot, illustrating the sequential triggering of flow from successively deeper sills.

[*White et al.*, 2011; *Pan et al.*, 1991; *Shelly and Hill*, 2011] and this may provide extra buoyancy force driving magma upwards in addition to the inter-sill pressure gradient.

3. Conclusions

[17] We attribute the progressive deepening of seismic activity to a decompression wave propagating down through the crust. This causes sequential depressurization of vertically separated magma reservoirs as melt from those reservoirs was mobilized and moved to the surface. This has key implications for hazard assessment of active volcanoes in interpreting details of the subsurface plumbing system, and of the inter-connections between sills at different crustal levels.

[18] **Acknowledgments.** Temporary seismometers used in this study are from the LOKI instrument pool, which is owned jointly by the Icelandic Meteorological Office, the Institute of Earth Sciences, University of Iceland and the Iceland GeoSurvey. We thank M. Hensch, S. Steinthórsson, T. Jónsson, Ó. Gudmundsson, B. Ófeigsson, the helicopter crew of the Icelandic Coast Guard and others who assisted with Eyjafjallajökull fieldwork. Generic Mapping Tools [*Wessel and Smith*, 1998] were used to produce some figures. J.T. is funded by a NERC studentship and CASE award supported by ERC Equipoise Ltd. We thank D. P. Hill and an anonymous reviewer for their comments. Department of Earth Sciences, Cambridge contribution number ESC2586.

[19] The Editor thanks David Hill and an anonymous reviewer for their assistance in evaluating this paper.

References

Drew, J. (2010), Coalescence microseismic mapping: An imaging method for the detection and location of seismic events, PhD dissertation, Univ. of Cambridge, Cambridge, U. K.

Gudmundsson, M. T., et al. (2012a), Summit eruption, in *The 2010 Eyjafjallajökull Eruption, Iceland*, edited by B. Thorkelsson et al., chap. 4.4, pp. 65–95, Icel. Meteorol. Off., Inst. of Earth Sci., Univ. of Icel., Reykjavík.

Gudmundsson, M. T., et al. (2012b), Ash generation and distribution from the April–May 2010 eruption of Eyjafjallajökull, Iceland, *Sci. Rep.*, *2*, 572, doi:10.1038/srep00572.

Hjaltadóttir, S., K. S. Vogfjörð, and R. Slunga (2009), Seismic signs of magma pathways through the crust in the Eyjafjallajökull volcano, south Iceland, *Rep. VI*, pp. 2009–2013, Icel. Meteorol. Off., Reykjavík.

Keiding, J. K., and O. Sigmarsson (2012), Geothermobarometry of the 2010 Eyjafjallajökull eruption: New constraints on Icelandic magma plumbing systems, *J. Geophys. Res.*, *117*, B00C09, doi:10.1029/2011JB008829.

Kelley, D. F., and M. Barton (2008), Pressures of crystallization of Icelandic magmas, *J. Petrol.*, *49*, 465–492, doi:10.1093/petrology/egm089.

Key, J., R. S. White, H. E. Soosalu, and S. S. Jakobsdóttir (2011), Multiple melt injection along a spreading segment at Askja, Iceland, *Geophys. Res. Lett.*, *38*, L05301, doi:10.1029/2010GL046264.

Magnússon, E., M. T. Gudmundsson, M. J. Roberts, G. Sigurðsson, F. Höskuldsson, and B. Oddsson (2012), Ice-volcano interactions during the 2010 Eyjafjallajökull eruption, as revealed by airborne imaging radar, *J. Geophys. Res.*, *117*, B07405, doi:10.1029/2012JB009250.

Pan, V., J. R. Holloway, and R. L. Hervig (1991), The pressure and temperature dependence of carbon dioxide solubility in tholeiitic basalt melts, *Geochim. Cosmochim. Acta*, *55*, 1587–1595, doi:10.1016/0016-7037(91)90130-W.

Rivalta, E., and P. Segall (2008), Magma compressibility and the missing source for some dike intrusions, *Geophys. Res. Lett.*, *35*, L04306, doi:10.1029/2007GL032521.

Shelly, D. R., and D. P. Hill (2011), Migrating swarms of brittle failure earthquakes in the lower crust beneath Mammoth Mountain, California, *Geophys. Res. Lett.*, *38*, L20307, doi:10.1029/2011GL049336.

Sigmarsson, O., et al. (2011), Remobilization of silicic intrusion by mafic magmas during the 2010 Eyjafjallajökull eruption, *Solid Earth*, *2*, 271–281, doi:10.5194/se-2-271-2011.

Sigmundsson, F., et al. (2010), Intrusion triggering of the 2010 Eyjafjallajökull explosive eruption, *Nature*, *468*, 426–430, doi:10.1038/nature09558.

Sturkell, E., F. Sigmundsson, and P. Einarsson (2003), Recent unrest and magma movements at Eyjafjallajökull and Katla volcanoes, Iceland, *J. Geophys. Res.*, *108*(B8), 2369, doi:10.1029/2001JB000917.

Tarasewicz, J., B. Brandsdóttir, R. S. White, M. Hensch, and B. Thorbjarnardóttir (2012), Using microearthquakes to track repeated magma intrusions beneath the Eyjafjallajökull stratovolcano, Iceland, *J. Geophys. Res.*, *117*, B00C06, doi:10.1029/2011JB008751.

Waldhauser, F., and W. L. Ellsworth (2000), A double-difference earthquake location algorithm: Method and application to the Northern Hayward Fault, California, *Bull. Seismol. Soc. Am.*, *90*(6), 1353–1368, doi:10.1785/0120000006.

Wessel, P., and W. H. F. Smith (1998), New, improved version of the Generic Mapping Tools released, *Eos Trans. AGU*, *79*(47), 579, doi:10.1029/98EO00426.

White, R. S., J. Drew, H. K. Martens, A. J. Key, H. Soosalu, and S. S. Jakobsdóttir (2011), Dynamics of dyke intrusion in the mid-crust of Iceland, *Earth Planet. Sci. Lett.*, *304*, 300–312, doi:10.1016/j.epsl.2011.02.038.

White, R. S., S. A. T. Redfern, and S.-Y. Chien (2012), Episodicity of seismicity accompanying melt intrusion into the crust, *Geophys. Res. Lett.*, *39*, L08306, doi:10.1029/2012GL051392.